IEEE Access
Multidisciplinary | Rapid Review | Open Access Journal

Received December 5, 2019, accepted December 19, 2019, date of publication December 30, 2019,
date of current version January 6, 2020.

Digital Object Identifier 10.1109/ACCESS.2019.2962841

Coordinated Planning With Predetermined Renewable Energy Generation Targets Using Extended Two-Stage Robust Optimization

KUNPENG TIAN[1], WEIQING SUN[2], DONG HAN[2], AND CE YANG[1]
[1]Department of Control Science and Engineering, University of Shanghai for Science and Technology, Shanghai 200093, China
[2]Department of Electrical Engineering, University of Shanghai for Science and Technology, Shanghai 200093, China

Corresponding author: Weiqing Sun (sidswq@163.com)

This work was supported by the National Natural Science Foundation of China under Grant 51777126.

ABSTRACT Coordinated planning is an effective method to balance investment costs and benefits in achieving high renewable target under the renewable-driven power system expansion wave. This paper proposes a coordinated planning model to support the efficient achievement of renewable target considering economy of the system by accounting for the interaction among source, grid, and energy storage system. An adaptive two-stage min-max-min robust optimization model is formulated to take into account renewable target as well as the uncertainty associated with renewable production and load demand. To reduce the conservatism of robust optimization, uncertain budget, multiple uncertain sets, and data-driven method are used to design uncertain sets. The resulting model is transformed into a tractable bi-level programming through strong duality theory and *big-M* method. A customized column-and-constraint generation algorithm is used to solve the bi-level programming. Simulation results presented for the modified IEEE 30-bus test system corroborates the effectiveness of the methodology, which finds siting and sizing of renewable energy sources and energy storage systems as well as transmission expansion schemes. It is capable to provide a flexible planning tool driven by renewable target under a reasonable computational burden.

INDEX TERMS
Coordinated planning, renewable target, two-stage robust optimization, multiple uncertain sets, data-driven, column-and-constraint generation algorithm.

NOMENCLATURE

SET

Ω_w	set of candidate wind turbines (WT)
Ω_{pv}	set of candidate photovoltaics (PV)
Ω_{es}	set of candidate energy storage systems (ESS)
Ω_l	set of candidate lines
Ω_g	set of all thermal generators (TG)
Ω_T	set of time periods
Ω_d	set of all loads

INDICES

i	index of nodes
t	index of hours
l	index of lines

The associate editor coordinating the review of this manuscript and approving it for publication was Guangya Yang.

PARAMETERS

c_w	annualized capital cost of candidate WT ($)
c_{pv}	annualized capital cost of candidate PV ($)
c_{es}	annualized capital cost of candidate ESS ($)
c_l	annualized capital cost of candidate lines ($)
$su_{g,i}$	the cost of start-up of TG at node i($)
$sd_{g,i}$	the cost of shut-down of TG at node i($)
$o_{g,i}$	the operation cost of TG at node ($/MWh)
o_d	penalty cost of unserved load demand ($/MWh)
N_w	maximum number of WT allowed to be built
N_{pv}	maximum number of PV allowed to be built
N_{es}	maximum number of ESS allowed to be built
N_l	maximum number of line allowed to be built
S_w	the capacity of WT units (MW)
S_{pv}	the capacity of PV units (MW)
ω	proportion of installed capacity of WT and PV
$T_{g,i}^{on}$	minimum on state duration of TG at node i (h)

$\hat{p}^t_{d,i}$ nominal estimate of load demand at node i during the t^{th} period (MW)
$\hat{p}^t_{w,i}$ nominal estimate of WT power production at node i during the t^{th} period (MW)
$\hat{p}^t_{pv,i}$ nominal estimate of PV power production at node i during the t^{th} period (MW)
$\eta_{es,c,i}$ efficiency of ESS at node i during charging
$\eta_{es,d,i}$ efficiency of ESS at node i during discharging
$r_{a,res}$ renewable energy targets
$r_{c,res}$ acceptable renewable energy spillage rate
$p^{\min}_{g,i}$ minimum production levels of TG at node i (MW)
$p^{\max}_{g,i}$ maximum production levels of TG at node i (MW)
$\Delta p^u_{g,i}$ ramp-up rate limit for TG at node i (MW/h)
$\Delta p^d_{g,i}$ ramp-down rate limit for TG at node i (MW/h)
p^d_{es} maximum discharging power of ESS units (MW)
p^c_{es} maximum charging power of ESS units (MW)
$e^{\min}_{es,i}$ minimum capacity of ESS units at node i (MWh)
$e^{\max}_{es,i}$ maximum capacity of ESS units at node i (MWh)
b_l susceptance of the line l (mho)
M_l a sufficiently large constant
$p^{\max}_{l,i}$ transmission capacity of the line l (MW)
gap convergence tolerance

VARIABLES

$C_{B,w}$ the investment costs of WT ($)
$C_{B,pv}$ the investment costs of PV ($)
$C_{B,es}$ the investment costs of ESS ($)
$C_{B,l}$ the investment costs of line ($)
$C_{O,g}$ the operation costs of the TG ($)
$C_{P,d}$ the penalty costs due to unserved load ($)
$n_{w,i}$ the number of WT at node i
$n_{pv,i}$ the number of PV at node i
$n_{es,i}$ the number of ESS at node i
x_l the status of candidate line l
$u^t_{g,i}$ start-up status of TG at node i during the t^{th} period
$v^t_{g,i}$ shut-down status of TG at node i during the t^{th} period
$p^t_{g,i}$ power production of TG at node i during the t^{th} period (MW)
$\Delta p^t_{d,i}$ load curtailment at node i during the t^{th} period (MW)
$s^t_{g,i}$ on/off state of TG at node i during the t^{th} period
τ auxiliary modeling variable
$p^t_{w,i}$ power production of WT at node i during the t^{th} period (MW)
$p^t_{pv,i}$ power production of PV at node i during the t^{th} period (MW)
$p^t_{es,i}$ auxiliary variable for ESS at node i during the t^{th} period (MW)
$p^t_{d,i}$ load demand at node i during the t^{th} period (MW)
$\Delta p^t_{w,i}$ spillage power of WT at node i during the t^{th} period (MW)
$\Delta p^t_{pv,i}$ spillage power of PV at node i during the t^{th} period (MW)
$p^t_{l,i}$ power flow of line connecting to node i during the t^{th} period (MW)
θ^t_i phase angles of nodes i during the t^{th} period
$p^t_{es,d,i}$ discharging power of ESS at node i during the t^{th} period (MW)
$p^t_{es,c,i}$ charging power of ESS at node i during the t^{th} period (MW)
$e^t_{es,i}$ state of charge for ESS at node i during the t^{th} period (MWh)
$s^t_{es,d,i}$ discharging status of ESS at node i during the t^{th} period
$s^t_{es,c,i}$ charging status of ESS at node i during the t^{th} period
$\tilde{p}^t_{d,i}$ uncertain load demand at node i during the t^{th} period (MW)
$\tilde{p}^t_{w,i}$ uncertain WT power production at node i during the t^{th} period (MW)
$\tilde{p}^t_{pv,i}$ uncertain PV power production at node i during the t^{th} period (MW)

VECTORS AND MATRICES

A, E, G, H, I matrices of coefficients
B, F, L vectors of requirements
C, D vectors of costs
$\hat{U}$ vector of nominal estimates for U
X discrete variable of investment and commitment related decisions
Y continuous variable of dispatch related decisions
U vector of uncertain variables

I. INTRODUCTION

A. BACKGROUND AND MOTIVATION

To relieve energy shortage and climate change, power systems worldwide are utilizing more energy from renewable energy sources (RES) such as wind power and photovoltaics [1]. The high penetration of RES has become the trend and important feature of the next generation power system [2]. To promote the development of RES and accelerate the transformation of energy structure, a series of policies have been implemented worldwide. In China, the renewable portfolio standard (RPS, the required fraction of power demand served by RES) was implemented in 2011 and strengthened since 2016 [3]. In the context of low carbon policies, RES as the core of generation expansion planning (GEP) recently has been drawing extensive attention in the power industry [4]. Different driving forces will lead to the failure of traditional expansion planning methods in the RPS framework. The traditional expansion planning is load-driven, which adapts to load growth and uses economic growth as a signal to forecast medium and long-term load. The future expansion planning is renewable-driven, in order to promote the transformation of energy structure and increase the fraction of power demand served by renewables [5].

Within this framework, the transmission systems and energy storage systems (ESS) play a key role in power systems planning and operation, allowing the policymakers to use the most economical investment to achieve the renewable target [6]. Both transmission systems and ESS can move power, the former moves power in spatially while the latter moves power in time [7]. Several scientific articles have highlighted the importance of coordinated planning to lower the cost of the investment. In [8], a continuous-time model based on stochastic and robust optimization technique is proposed to coordinate the transmission expansion planning (TEP) and energy storage investment. Reference [9] points out that the lack of coordinated planning of wind turbine (WT) and expansion of the transmission systems may lead to curtailment of wind power due to operational constraints. Reference [10] proposes a coordinated operational dispatch scheme, which can reduce the impacts of wind power forecast errors while prolonging the lifetime of ESS. Reference [11] proposes a coordinated planning model for power systems with regulation capacity constraints being taken into account to deal with wind power curtailment. Reference [12] presents a model to decide the joint expansion planning of distributed generation and the distribution network considering the impact of ESS and price-dependent demand response. For a predetermined renewable target, research on coordinated planning of power system considering the interaction of source, grid and ESS is seldom in existing literatures.

On the other hand, the uncertainties of RES production and load demand are important point at the time of determining decisions [13]. There have been several reported attempts to account for uncertainty in the planning formulation. Stochastic optimization (SO) uses scenario representation to express systems uncertainties. Reference [14] shows the application of stochastic mixed-integer line programming (MILP) to account for hydrological uncertainty in GEP. However, it is difficult to identify the exact probability density function for random variables. Robust optimization (RO) uses boundaries to model uncertainties. Accordingly, RO needs less historical data of uncertain parameters than SO [15]. Reference [16] proposed a power flow control method using smart wire devices (SWD) to promote large-scale wind energy penetration. The SWD placement problem is formulated as an adaptive robust optimization (ARO) problem with three-levels. In practical applications, it is necessary to select appropriate methods to deal with uncertainty based on scenarios.

In this paper, the problem of coordinated planning and operation of renewable-driven power systems has been focused on. From static planning, considering the dynamic operating characteristics of the power systems, a source, grid, and ESS coordinated planning model suitable for different stages of RES development is established. The model considers two stages of power systems planning and operation, and combines SO and RO techniques. Uncertain budgets, multiple uncertain sets, and data-driven technologies are used to describe the uncertainty associated with renewable production and load demand to reduce the conservativeness of decision-making. Mathematically, the adaptive two-stage robust optimization model has a three-level structure of min-max-min. Based on the column-and-constraint generation algorithm (C&CG) framework, the ARO problem is decomposed into master problems (MP) and subproblems (SP), and the SP are recast to single-level for MILP using strong duality theory and *Big-M* method.

B. CONTRIBUTIONS

The main contributions of the paper can be summarized as follows:

1) A novel two-stage min-max-min coordinated planning framework for co-optimizing the siting and sizing of RES and ESS as well as transmission expansion to meet renewable target under the uncertainties of RES production and load demand. Besides, this framework integrates a variety of uncertainty modeling techniques to constitute a tradeoff between accuracy and tractability.

2) The value of RES production is influenced by many factors, such as environmental protection concepts and technology. This result leads to differences in the temporal and spatial of renewable energy targets. Therefore, the accommodation and curtailment of renewable energy are taken as constraint conditions. With this setting, our research as a tool can provide a planning scheme to meet the predetermined renewable energy targets.

C. PAPER ORGANIZATION

The remainder of this paper is organized as follows. Section II describes the main problem and corresponding methods of planning with RPS. In Section III, a detailed deterministic coordinated programming model is proposed. In Section IV, the mathematical formulations of adaptive two-stage robust models are described and a customized algorithm is given. In Section V, the proposed ARO model is tested on the modified IEEE 30-bus test system and the obtained numerical results are discussed extensively. Finally, relevant conclusions are drawn in Section VI.

II. PROBLEM DESCRIPTION

A. APPROACH OF COORDINATED PLANNING

This paper focuses on static planning, aiming at joint optimizing the siting and sizing of RES and ESS as well as transmission expansion scheme. Coordinated planning includes the following two aspects. Firstly, complementary resources such as source, grid, and ESS. GEP improves penetration to meet renewable target. TEP improves the transmission capacity to adapt to the increase of load and renewable. ESS has a significant effect on mitigating uncertainty and line congestion. Co-optimizing source, grid, and ESS investment allow cost savings [17]. Secondly, a unified framework for power system planning and operation. The combination of power system planning and operation is one of the key technologies to meet renewable target and lower investment costs. Sequential production simulation is applied to describe

the time series characteristics of RES production and load demand [18]. The proposed multi-period static planning tool can be simply extended to become a dynamic approach at the expense of a higher computation burden [19]. Ignoring the dynamic balance characteristics of power systems with high penetration of RES will lead to renewable spillage and load curtailment, and the renewable target will be threatened.

B. MULTIPLE UNCERTAINTY SETS

Since the proposed model solves joint planning and operation problems depends on the daily load demand and RES production profiles, it is required to model uncertainties of load demand and RES production profiles throughout a daily period. Considering the computation burden and accuracy of the model, the two-stage ARO technique is used to deal with the uncertainty of RES production and load demand power. In general, the solutions of RO approaches are often too conservative and pessimistic, which may lead to high system costs. Such a result is due to the underutilization of historical data in describing the uncertainties of RES and load. Therefore, uncertain sets need to be carefully designed. To address the issue, [20] considers the weighted summation of performances over multiple uncertainty sets and applies to the unit commitment problem. Such a classical RO problem can be considered as $F = \min \max f(x, u)$, where x and u are decision variables and uncertain variables respectively. Assume that there are multiple uncertain sets and satisfy $U_1 \subseteq U_2 \subseteq \ldots \subseteq U_K$, and denote their corresponding optimal values of $F(U_1)$, $F(U_2)\ldots$and $F(U_K)$. We have $F(U_1) \leq F(U_2)\ldots \leq F(U_K)$. Weight coefficients are assigned to each uncertain set, such as a set of coefficients $p_1, p_2, \ldots, p_K$ with $p_1 + p_2 + \ldots + p_K = 1$. The uncertain sets in RO are similar to the scenarios in SO, and the coefficients corresponding to uncertain sets are similar to the probability of scenarios occurring. The weighted values of the objective function under multiple uncertain sets are calculated to reduce the impact of unrealistic worst-case situations in line with the previous research works [20]. In this paper, the uncertainty in daily RES production and load demand profiles are modeled using a data-driven method. We consider the correlation and uncertainty budget to construct accurate uncertain sets and employ multiple uncertain sets to reduce the impact of unrealistic worst-case situations.

C. DATA-DRIVEN MODEL

In this section, we provide one approach to construct uncertain sets based on confidence bands for cumulative distribution function (CDF) from nonparametric statistics. The uncertain set modeling method includes two steps: the confidence band of CDF is constructed, and the confidence band of CDF is transformed into an uncertain set [21]. Nonparametric statistics does not involve the parameters describing the population distribution and so that called distribution-free. The standard nonparametric estimate of the population CDF is based on Kolmogorov-Smirnov (K-S) statistic [22]. However, the K-S test does not provide uniform sensitivity in different

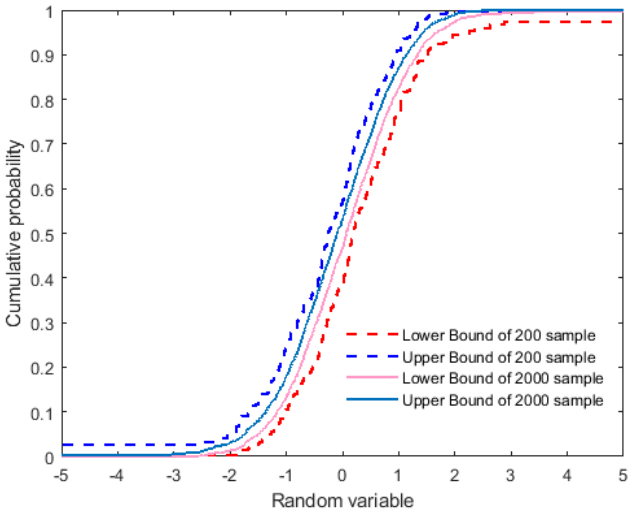

FIGURE 1. Confidence bands of CDF constructed from different size samples.

parts of the distribution. Therefore, the confidence band of CDF is obtained by the Dirichlet method. Reference [23] provides the detailed process of deriving finite sample confidence bands of CDF based on the Dirichlet method. The convergence property of the confidence bands becomes more and more narrowed as the size of the sample set grows, as shown in Figure 1.

For the given confidence level β and ascendingly ordered historical data set $\Omega_{data} = \{\xi_1, \xi_2, \xi_3 \ldots, \xi_h\}$, define $f_a^{ub}(x) = B_{a,h}^{\tilde{\beta}/2}$ and $f_a^{lb}(x) = B_{a,h}^{1-\tilde{\beta}/2}$, where a is the sequential index of historical data, $B_{a,h}^{\tilde{\beta}/2}$ represents the $\tilde{\beta}/2$-quantile of distribution function $B(a, h+1-a)$, $\tilde{\beta}$ is a parameter related to confidence level and sample size, and the calculation formula is given in [23]. Suppose that $\bar{F}(x)$ and $\underline{F}(x)$ are the upper and lower bounds of CDF, and we can get the β-confidence band for CDF, $\bar{F}(x) = \min\left\{f_a^{ub} : \xi_a \leq x\right\}$ and $\underline{F}(x) = \max\left\{f_a^{lb} : \xi_a \leq x\right\}$. Note that confidence bands for CDF do not contain the true information of the random variable. The interval of the random variable can be estimated according to the probability points on the CDF confidence band. The upper bound of the true value $\bar{x} = \min\{x{:}\underline{F}(x) \geq (1-\beta)/2\}$, and the lower bound of the true value $\underline{x} = \max\{x{:}\bar{F}(x) \leq (1+\beta)/2\}$. Researches show that with the increase of historical data, the CDF approaches the real distribution [21]. In summary, the data-driven uncertain set modeling process is as Algorithm 1.

This method can be used to estimate the power intervals of RES and load at different sample sizes and confidence levels. Unlike the scenario-based uncertainty set modeling method [24], the distribution information and confidence level are considered in the process of modeling a single uncertain set. We note that a systematic data-driven approach based on Dirichlet process mixture model to construct an uncertainty set is presented in [25]. The applicability of the methods mentioned above will be given fully consideration in our future works with different scenes. Besides, [26] proposed applies

Algorithm 1 Data-Driven Modeling Algorithms

1. Collect historical data and calculate order statistics, set confidence level β.
2. For a given historical data size and confidence level, the parameter of Beta distribution is calculated according to the equation in [23].
3. The upper and lower confidence bounds for CDF are obtained by calculating the quantile of Beta distribution.
4. Estimated the interval range of the true value of the random variable according to the probability points on the CDF confidence band.

the kernel density estimation to establish an ambiguity set of continuous multivariate probability distributions, in which the selection of bandwidth is very important.

III. DETERMINISTIC COORDINATED PROGRAMMING MODEL

Following the modeling framework of power systems static planning, the deterministic coordinated programming problem can be formulated using the following MILP model. As a daily time horizon can adequately model the dynamics and cyclic behaviors of power systems, a daily time horizon is considered in this work.

A. OBJECTIVE FUNCTION

The objective function of the joint source, grid, and ESS planning problem is to minimize investment and operation costs. The operating cost consists of start-up cost, shutdown cost, fuel cost and penalty cost of the unserved load.

$$\min \quad C_{B,w} + C_{B,pv} + C_{B,es} + C_{B,l} + C_{O,g} + C_{P,d} \tag{1}$$

$$C_{B,w} = \sum_{i\in\Omega_w} c_w n_{w,i} \tag{2}$$

$$C_{B,pv} = \sum_{i\in\Omega_{pv}} c_{pv} n_{pv,i} \tag{3}$$

$$C_{B,es} = \sum_{i\in\Omega_{es}} c_{es} n_{es,i} \tag{4}$$

$$C_{B,l} = \sum_{l\in\Omega_l} c_l x_l \tag{5}$$

$$C_{O,g} = \sum_{t\in\Omega_T} \left(\sum_{i\in\Omega_g} su_{g,i} u^t_{g,i} + \sum_{i\in\Omega_g} sd_{g,i} v^t_{g,i} + \sum_{i\in\Omega_g} o_{g,i} p^t_{g,i} \right) \tag{6}$$

$$C_{P,d} = \sum_{t\in\Omega_T} \sum_{i\in\Omega_d} o_d \Delta p^t_{d,i} \tag{7}$$

Equations (2)-(5) represent investment of WT, photovoltaic (PV), ESS, and transmission lines, respectively. Operational costs of the ESS, such as degradation cost, operation and maintenance cost, are converted to daily cost in a fixed proportion. Equation (6) represents operation costs of TG. Equation (7) represents penalty costs of the unserved load.

B. CONSTRAINTS

In addition to the traditional technical and operational constraints, RES accommodation and spillage constraints should be satisfied.

$$\sum_{i\in\Omega_w} n_{w,i} \le N_w \tag{8}$$

$$\sum_{i\in\Omega_{pv}} n_{pv,i} \le N_{pv} \tag{9}$$

$$\sum_{i\in\Omega_{es}} n_{es,i} \le N_{es} \tag{10}$$

$$\sum_{l\in\Omega_l} x_l \le N_l, \quad x_l \in \{0,1\} \tag{11}$$

Equations (8)-(11) limit the maximum number of WT, PV, ESS, lines allowed to be built.

$$\sum_{i\in\Omega_w} n_{w,i} S_w = \omega \sum_{i\in\Omega_{pv}} n_{pv,i} S_{pv} \tag{12}$$

Equation (12) limits proportion of installed capacity of WT and PV to develop renewable energy reasonably.

$$s^{t-1}_{g,i} - s^t_{g,i} + u^t_{g,i} \ge 0 \tag{13}$$

$$s^t_{g,i} - s^{t-1}_{g,i} + v^t_{g,i} \ge 0 \tag{14}$$

Equations (13) and (14) are logic constraints between on and off status and the turn-on and turn-off actions.

$$-s^t_{g,i} + s^{t-1}_{g,i} + u^\tau_{g,i} \ge 0, \quad \tau \in [t+1, \min\left\{t + T^{on}_{g,i} - 1, T\right\}] \tag{15}$$

$$-s^{t-1}_{g,i} + s^t_{g,i} - v^\tau_{g,i} \ge 1, \quad \tau \in [t+1, \min\left\{t + T^{down}_{g,i} - 1, T\right\}] \tag{16}$$

Equations (15) and (16) describe the minimum up and minimum down time restrictions, respectively.

$$p^t_{g,i} + p^t_{w,i} - \Delta p^t_{w,i} + p^t_{pv,i} - \Delta p^t_{pv,i} + p^t_{es,i} + p^t_{l,i} = p^t_{d,i} - \Delta p^t_{d,i} \tag{17}$$

Equation (17) represents nodal power balance.

$$p^t_{d,i} = \tilde{p}^t_{d,i} \tag{18}$$

Equation (18) represents the uncertainty of load demand.

$$0 \le \Delta p^t_{w,i} \le p^t_{w,i} \tag{19}$$

$$0 \le \Delta p^t_{pv,i} \le p^t_{pv,i} \tag{20}$$

$$0 \le \Delta p^t_{d,i} \le p^t_{d,i} \tag{21}$$

Equations (19)-(21) bound the maximum spilled RES productions power and unserved load demands at all nodes.

$$p^t_{es,i} = p^t_{es,d,i} - p^t_{es,c,i} \tag{22}$$

$$e^t_{es,i} = e^{t-1}_{es,i} + p^t_{es,c,i} \eta_{es,c,i} - p^t_{es,d,i} / \eta_{es,d,i} \tag{23}$$

$$\sum_{t\in\Omega_T}\left(p^t_{es,i,c}\eta_{es,i,c}-p^t_{es,i,d}/\eta_{es,i,d}\right)=0 \tag{24}$$

Equation (24) represents the operation strategy of ESS and binds the initial and final stored energy levels of each ESS in every representative day.

$$\sum_{t\in\Omega_T}\left\{\sum_{i\in\Omega_w}\left(p^t_{w,i}-\Delta p^t_{w,i}\right)+\sum_{i\in\Omega_{pv}}\left(p^t_{pv,i}-\Delta p^t_{pv,i}\right)\right\} = r_{a,res}\sum_{t\in\Omega_T}\sum_{i\in\Omega_d}\left(p^t_{d,i}-\Delta p^t_{d,i}\right) \tag{25}$$

Equation (25) imposes an amount of RES sharing in the demand supply defined by the parameter $r_{a,res}$ which can be set to a value between 0 and 1.

$$\sum_{t\in\Omega_T}\left\{\sum_{i\in\Omega_w}\Delta p^t_{w,i}+\sum_{i\in\Omega_{pv}}\Delta p^t_{pv,i}+\sum_{i\in\Omega_{es}}\Delta p^t_{es,i}\right\} \le r_{c,res}\sum_{t\in\Omega_T}\left\{\sum_{i\in\Omega_w}p^t_{w,i}+\sum_{i\in\Omega_{pv}}p^t_{pv,i}\right\} \tag{26}$$

Equation (26) imposes a maximum amount of RES spillage defined by the parameter $r_{c,res}$ which can be set to a value between 0 and 1, and the loss of ESS is calculated as a renewable spillage. Equations (25)-(26) can be selected according to the preferences of decision makers in practical applications. The accommodation targets and spillage rates of RES vary in different regions and periods. Adding renewable target to constraints instead of setting penalties term in the objective function can improve the applicability of the model.

$$p^{\min}_{g,i}s^t_{g,i}\le p^t_{g,i}\le p^{\max}_{g,i}s^t_{g,i} \tag{27}$$

Equation (27) limits the production power for all TG.

$$p^t_{g,i}-p^{t-1}_{g,i}\le\Delta p^u_{g,i}s^{t-1}_{g,i}+p^{\min}_{g,i}(s^t_{g,i}-s^{t-1}_{g,i}) \tag{28}$$

$$p^{t-1}_{g,i}-p^t_{g,i}\le\Delta p^d_{g,i}s^t_{g,i}+p^{\min}_{g,i}(s^{t-1}_{g,i}-s^t_{g,i}) \tag{29}$$

Equations (28) and (29) limit the ramp-up and ramp-down of TG, respectively. It is worth mentioning that the start-up power of TG is set to the minimum production levels.

$$p^t_{w,i}=n_{w,i}S_w\tilde{p}^t_{w,i} \tag{30}$$

$$p^t_{pv,i}=n_{pv,i}S_{pv}\tilde{p}^t_{pv,i} \tag{31}$$

Equations (30) and (31) represent the uncertainty of WT and PV production, respectively.

$$0\le p^t_{es,d,i}\le n_{es,i}s^t_{es,d,i}p^d_{es} \tag{32}$$

$$0\le p^t_{es,c,i}\le n_{es,i}s^t_{es,c,i}p^c_{es} \tag{33}$$

Equations (32) and (33) denote the maximum discharging and charging limits of ESS, respectively.

$$s^t_{es,d,i}+s^t_{es,c,i}\le 1 \tag{34}$$

Equation (34) prevents that ESS simultaneously charges and discharges [27]. Actually, this constraint is redundant when charging and discharging efficiency are considered.

$$n_{es,i}e^{\min}_{es,i}\le e^t_{es,i}\le n_{es,i}e^{\max}_{es,i} \tag{35}$$

Equation (35) represents limit the stored energy of ESS during each period.

$$\left|p^t_{l,i}-b_l(\theta^t_i-\theta^t_j)\right|\le M_l(1-x_l) \tag{36}$$

Equation (36) models the DC power flow approach to describe the line flows in terms of nodal voltage angles for all lines. A sufficiently large constant M_l used to form disjunctive constraints as described in [13].

$$-x_lp^{\max}_{l,i}\le p^t_{l,i}\le x_lp^{\max}_{l,i} \tag{37}$$

Equation (37) establishes power flow capacity limits for all transmission lines.

$$\tilde{p}^t_{w,i}=\hat{p}^t_{w,i} \tag{38}$$

$$\tilde{p}^t_{pv,i}=\hat{p}^t_{pv,i} \tag{39}$$

$$\tilde{p}^t_{d,i}=\hat{p}^t_{d,i} \tag{40}$$

Equations (38)-(40) indicate that the power of WT, PV, and load demand are fixed on their nominal estimates.

The deterministic formulation of (1)-(40) can be rewritten in a compact form as follows:

$$\min_{X,Y}\ C'X+D'Y \tag{41}$$

$$AX\ge B \tag{42}$$

$$EY\ge F \tag{43}$$

$$GX+HY\ge L \tag{44}$$

$$IY=\hat{U} \tag{45}$$

Equation (42) corresponds to (8)-(16), equation (43) corresponds to (17)-(26), equation (44) corresponds to (27)-(37), and equation (45) corresponds to (38)-(40). The deterministic coordinated planning model of (41)-(45) is a MILP problem, which can be solved directly by commercial software to obtain the siting and sizing of RES and ESS as well as the transmission expansion scheme. The optimal solution cannot resist arbitrarily realizations of the uncertain RES power productions and load demands as the predicted power is fixed on their nominal estimates.

IV. EXTENDED ROBUST COORDINATED PROGRAMMING MODEL

A. DEFINITION OF UNCERTAINTY SETS

In this paper, we consider uncertainties associated with RES production power and load demands. The polyhedral set with a budget of uncertainty is shown as below [28].

$$U=\left\{\begin{array}{l}\tilde{u}^t_i|\tilde{u}^t_i=\left(\bar{u}^t_i-\hat{u}^t_i\right)\bar{z}^t_i+\left(u^t_i-\hat{u}^t_i\right)\underline{z}^t_i+\hat{u}^t_i\\ \bar{z}^t_i+\underline{z}^t_i\le 1\\ \sum\limits_i\left(\bar{z}^t_i+\underline{z}^t_i\right)\le\Gamma_s\\ \sum\limits_t\left(\bar{z}^t_i+\underline{z}^t_i\right)\le\Gamma_t\end{array}\right\} \tag{46}$$

where $\bar{u}^t_i$ and $\underline{u}^t_i$ are the upper and lower bounds of uncertain variable. $\bar{z}^t_i$ and $\underline{z}^t_i$ are binary auxiliary variable. Γ_s and Γ_t have used controls the number of uncertain parameters

that can deviate from their nominal value employing norm-1 constraints imposed on the error vectors. Specifically, Γ_s is restricts the correlation of WT in spatially, and Γ_t is restricts the correlation of WT in time. Further, the size of the uncertainty set U is controlled by Γ_s and Γ_t [29]. Although the uncertainty set only contains the extremum information of historical data and ignores the distribution information of historical data, the cumulative distribution information of historical data is considered in the modeling process of uncertainty set. The data-driven modeling technology based on historical data can obtain more accurate uncertainty sets and reduce the conservatism of robust optimization.

B. TWO STAGE ROBUST OPTIMIZATION MODEL

Coordinated planning considering the uncertainty of RES production power and load demands has two-stage decision-making nature. The investment decision and commitment related decisions are determined in a *here-and-now* manner before the uncertainty is realized. The economic dispatch decisions are assumed to be *wait-and-see* made after the observation of uncertain outcomes. Suppose that the uncertain sets under K confidence levels are U_1, U_2, …, U_{K} and σ_1, σ_2, …σ_{K} are their weight coefficients normalized for the totality being one. The complete three-level robust optimization model is formulated accordingly:

$$\min \quad C'X + \sum_k \sigma_k \left(\max_{\xi \in U_k} \min D_k' Y_k \right) \tag{47}$$

$$AX \geq B \tag{48}$$

$$E_k Y_k \geq F_k \tag{49}$$

$$G_k X + H_k Y_k \geq L_k \tag{50}$$

$$I_k Y_k = \tilde{U}_k \tag{51}$$

where the second stage is a max-min problem, which aims to seek the worst scenario economic dispatching scheme for a given set of uncertain sets. Note that constraints (49)-(51) are indexed with k, and the number of uncertain sets determines the number of constraints. Each uncertain set U_k corresponds to a Y_k. Thus, considering multiple uncertain sets will increase the computational pressure. Reference [20] has discussed this issue, and the increased computational burden is mild. Besides, although there is no rigorous statistical analysis, we are convinced that the worst-case scenario is more likely to occur in uncertain sets with higher confidence levels. We can show our confidence by setting the values of different weight coefficients to achieve the desired trade-off between cost and risk. We note that the feasible domain of Y_k is affected by the decision variables of the first stage and that the decision of the second stage has a max-min structure. A two-stage robust optimization problem with a three-level structure cannot be solved directly by commercial software. Customization of the C&CG based on the master-subproblem algorithm framework is used to solve this problem [30].

C. SOLUTION METHODOLOGY

Since the C&CG decomposition method has a two-level structure, the first step is to reformulate the inner max-min problem to a single-level optimization problem use strong duality theory. For a given X_0, we define the following SP:

$$Q\left(X^0\right) = \sum_k \sigma_k \left(\max_{\xi \in U_k} \min D_k' Y_k \right) \tag{52}$$

$$E_k Y_k \geq F_k \tag{53}$$

$$H_k Y_k \geq L_k - G_k X^0 \tag{54}$$

$$I_k Y_k = \tilde{U}_k \tag{55}$$

Solving $Q(x_0)$ is equivalent to solving the following dual problem:

$$\begin{aligned} \max \ & \sum_k \Psi_k F_k + \Pi_k \left(L_k - G_k X^0 \right) + \Upsilon_k \tilde{U}_k \\ s.t. \ & E_k' \Psi_k + H_k' \Pi_k + I_k' \Upsilon_k \leq \sigma_k D_k \\ & \Psi_k \geq 0, \quad \Pi_k \geq 0, \ \Upsilon_k \in R, \ k \in 1, 2 \ldots, K \end{aligned} \tag{56}$$

where Ψ_k, Π_k and Υ_k are dual variables for constraints (53)-(55). The dual problem caused by $\Upsilon_k \tilde{U}_k$ in objective function is an intractable bilinear problem. It is known that the optimal solution of the dual problem is on a vertex of the uncertain set [31], and the optimal solution can be obtained by searching all vertexes of uncertain set. Therefore, the dual problem (56) can be rewritten by using (46) as follows:

$$\begin{aligned} \max & \sum_k \Psi_k F_k + \Pi_k \left(L_k - G_k X^0 \right) \\ & + \Upsilon_k \bar{Z}_k \left(\bar{U}_k - \hat{U}_k \right) + \Upsilon_k Z_k \left(U_k - \hat{U}_k \right) + \Upsilon_k \hat{U}_k \\ s.t. \ & E_k' \Psi_k + H_k' \Pi_k + I_k' \Upsilon_k \leq \sigma_k D_k \\ & \bar{z}_{i,k}^t + \underline{z}_{i,k}^t \leq 1 \\ & \sum_i \left(\bar{z}_{i,k}^t + \underline{z}_{i,k}^t \right) \leq \Gamma_{s,k} \\ & \sum_t \left(\bar{z}_{i,k}^t + \underline{z}_{i,k}^t \right) \leq \Gamma_{t,k} \\ & \Psi_k \geq 0, \quad \Pi_k \geq 0, \ \Upsilon_k \in R, \\ & \bar{Z}_k \in \{0,1\}, \quad \underline{Z}_k \in \{0,1\}, \ k \in 1, 2 \ldots, K \end{aligned} \tag{57}$$

However, objective function still includes non-linear terms due to multiplication of the binary variables $\bar{Z}_k$ and $\underline{Z}_k$ (i.e., $\bar{z}_{i,k}^t$ and $\underline{z}_{i,k}^t$, respectively) and the continuous variable Υ_k. The non-linear terms $\Upsilon_k \bar{Z}_k$ and $\Upsilon_k \underline{Z}_k$ can be linearized in terms of new auxiliary variables $\bar{J}_k$ and $\underline{J}_k$, respectively.

$$\begin{aligned} \max \ & \bar{J}_k \left(\bar{U}_k - \hat{U}_k \right) + \underline{J}_k \left(U_k - \hat{U}_k \right) \\ s.t. \ & -\bar{Z}_k M_k \leq \bar{J}_k \leq \bar{Z}_k M_k \\ & \left| \bar{J}_k - \Upsilon_k \bar{Z}_k \right| \leq \left(1 - \bar{Z}_k\right) \bar{M}_k \\ & -Z_k M_k \leq \underline{J}_k \leq Z_k M_k \\ & \left| \underline{J}_k - \Upsilon_k Z_{kk} \right| \leq (1 - Z_k) \underline{M}_k \end{aligned} \tag{58}$$

where $\bar{M}_k$ and $\underline{M}_k$ are sufficiently large constant. Finally, the SP is reformulate as a tractable MILP. The objective

function values and the worst-case in each uncertain set are obtained by solving sub-problems, assuming that the optimal solutions of the v^{th} iteration are Q^v and $\tilde{U}_k^v$. On the other hand, the MP can be written as follows:

$$\begin{aligned} \min \quad & C'X + \eta \\ s.t. \quad & AX \geq B \\ & \eta \geq \sum_k \sigma_k D_k' Y_k^{l_k} \\ & E_k Y_k^{l_k} \geq F_k \\ & G_k X + H_k Y_k^{l_k} \geq L_k \\ & I_k Y_k^{l_k} = \tilde{U}_k^{l_k} \\ & 1 \leq l_k \leq v, \quad k \in 1, 2 \ldots, K \end{aligned} \tag{59}$$

where constraints with index l_k are cutting planes generated by SP. The recourse decision variables are created in each iteration, and the whole procedure is a column-and-constraint generation procedure. Although considering K uncertain sets will increase the number of variables and constraints in SP by K times. However, for a given X^0, the constraints in the SP are independent, so the parallel algorithm can be used to solve the problem. The flow chart is shown in Figure 2.

The specific solution process is as follows:

Algorithm 2 Column-and-Constraint Generation Algorithm

1. Initialization: Set $LB = inf$, $UB = sup$, $v = 0$, $k = 1$, 2, …, K, gap = 0.001.
2. Solve the MP to derive an optimal solution of first stage and update $LB = C'X^v + \eta^v$, $v = v+1$.
3. With given X^v, for $k = 1, 2, \ldots K$, do
   a) Solve the SP to identify worst-case and update $UB = \min\{UB, C'X^v + Q(X^v)\}$.
   b) Create recourse decision variables in the forms of constraints of the recourse problem.
4. If UB-$LB \leq$ gap, return X^{v+1} and end. Otherwise, add the cutting plane in MP and go to Step 2.

V. NUMERICAL STUDIES

In this section, the proposed coordinated planning considering multiple uncertain sets is implemented on the modified IEEE 30-bus test system [32]. The numerical examples are implemented in MATLAB 2018a with Gurobi as the MILP solver, and run on a 3.5GHz Intel Xeon(R) Gold 6135M processor with 48 GB RAM and 64-bit Windows 10 system. The average computation time for each scheme of the IEEE 30-bus test system is around 10 minutes, which is acceptable for offline calculation. Firstly, the modified test system data and parameter settings are given in Section V-A. Secondly, the impact of renewable target on planning schemes and the advantages of coordinated planning is analyzed in Section V-B. Finally, we study the effect of uncertain sets on the planning scheme and verify the effectiveness of the proposed model.

TABLE 1. Parameters for thermal generator.

No.(Bus)	G1(1)	G2(2)	G3(13)	G4(22)	G5(23)	G6(27)
P_{max}(MW)	80	80	40	50	30	55
P_{min}(MW)	24	24	12	15	9	16.5
T_{on}(h)	4	3	2	3	2	1
T_{off}(h)	4	3	2	2	1	1
Ramp(MW/h)	8	8	4	5	0	0
Cost($/MWh)	40	45	50	65	55	60
Star-up($)	300	260	200	320	260	220

TABLE 2. Parameters of candidate ESS.

Charge(MW)	Discharge(MW)	Capacity(MWh)	Cost/(k$/MWh)
100	100	200	570

A. PARAMETER SETTINGS

The modified systems has 30 nodes that are connected through 41 transmission lines, and the parameter of lines are given Table 7. The parameters of TG are shown in Table 1.

The renewable target is set as 10%, WT and PV installed capacity is set equal. The maximum load demand in the modified systems is two times of their original values and the unserved load cost is 50 k$/MWh. The investment cost of the line is 50 k$/km and the life span is 20 years. The capacity of each candidate WT and PV unit is 5 MW and 3 MW, respectively. The life span of WT and PV is 20 year, and the investment cost is 500 k$/MW and 800 k$/MW, respectively. The parameters of candidate ESS are given in Table 2. The scheduling period is 24 h and the time plot is 1 hour. The daily capital cost of candidate generation and line are obtained by applying the capital recovery factor (i.e., 6%).

The basic scenario of RES and load are clustered according to historical data, as shown in Figure 3.

B. ADVANTAGES OF COORDINATED PLANNING

The coordinated planning considering the interaction of source, grid and ESS can effectively reduce the investment cost in the same renewable target. The following schemes are tested as follows:

Schemes 1: coordinated planning considering RES, transmission lines, and ESS.

Schemes 2: coordinated planning considering RES and ESS, without transmission lines (namely $N_l = 0$).

Schemes 3: coordinated planning considering RES and transmission lines, without ESS (namely $N_{es} = 0$).

Note that the RES curtailment rate constraint (26) is ignored and constraint (25) is considered. Uncertain budget parameters for WT, PV, and load are set to zero. The planning results are shown in Table 3. Outside brackets are candidate nodes, and inside brackets are the quantity of ESS, WT, and PV units.

The power production of RES in schemes is 763.2 MWh. In *Scheme 1*, the installed capacity and spillover of RES are 90 MW and 126.1 MWh, respectively. In *Scheme 2*,

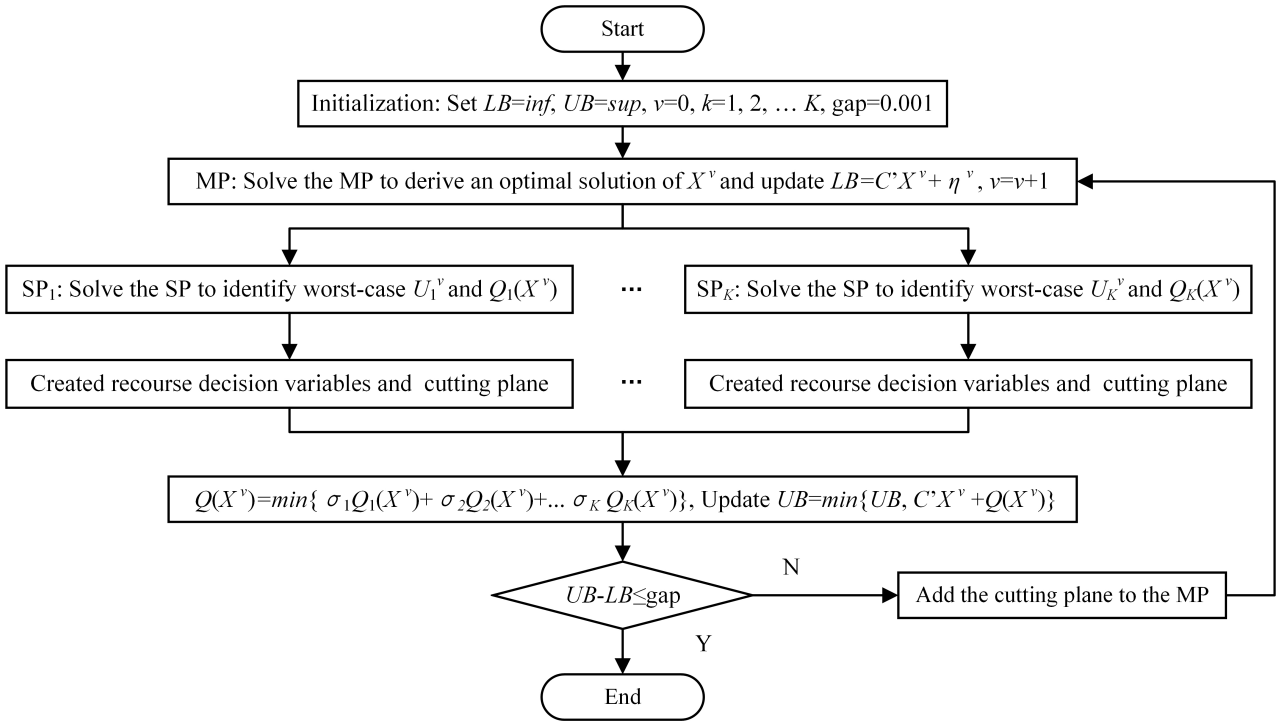

FIGURE 2. The outline of the parallel C&CG algorithm.

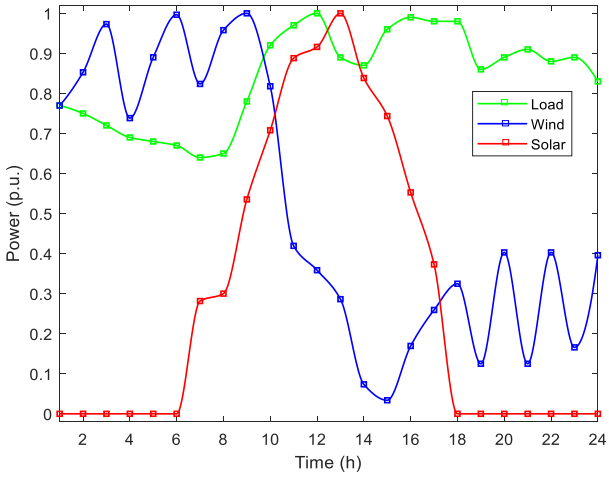

FIGURE 3. WT, PV and load power curves in basic scenarios.

the installed capacity and spillover of RES are 150 MW and 709.6 MWh, respectively. In *Scheme 3*, the installed capacity and spillover of RES are 240 MW and 1576.8 MWh, respectively. The daily investment costs of the three planning schemes are 25452 $, 35148 $ and 39500 $, respectively. The daily costs of the schemes are given in Table 4.

The data in the table indicate that *Scheme 1* is the optimal planning scheme with the same renewable target. Thermal generator start-up and shutdown can provide ramp-up and ramp-down capacity to reduce investment costs. The scheduling plan of TG in *Scheme 1* is shown in Figure. 4.

Low-cost generators bear the main power supply loads (such as G1 and G2) while high-cost generators are used for peak shaving (such as G4 and G5). Load demand continued to decline in the 3^{rd} to 7^{th} period, the G3 with the lowest start-up cost was shutdown to push the consumption of RES. If any TG is also shutdown in *Scheme 2* and *Scheme 3*, then there will be a penalty cost of the unserved load or more investment costs as the interaction of source, grid, and ESS is ignored. Generators with fast start-up and shutdown capability can

TABLE 3. Comparison of schemes in same renewable target.

	Scheme 1	*Scheme 2*	*Scheme 3*
Line	6-8, 21-22, 25-27	-	6-8, 21-22, 28-27
ESS	15(3), 17(2), 25(2), 26(2), 30(2)	8(5), 15(3), 21(4), 30(2)	-
WT	15(5), 18(2), 20(2)	8(11), 21(4)	8(11), 15(7), 21(2), 24(2), 26(2)
PV	8(3), 15(6), 21(4), 24(2)	8(8), 14(2), 15(3), 21(10), 26(2)	8(38), 26(2)

TABLE 4. Daily costs comparison of schemes in same renewable target.

Cost($)	*Scheme 1*	*Scheme 2*	*Scheme 3*
Line	2150	0	2269
ESS	9334	11877	0
WT	5373	8949	14323
PV	8595	14323	22908
Fuel	341140	337879	338706
Start-up	1760	1560	1560
Penalty	0	0	0
Total	368352	374588	379766

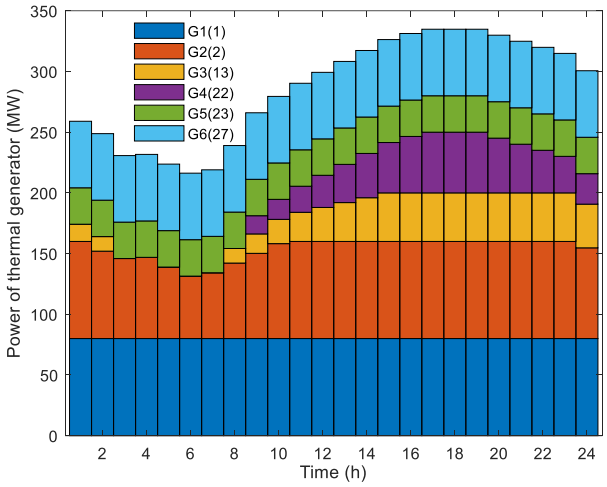

FIGURE 4. Production power of TG in Scheme 1.

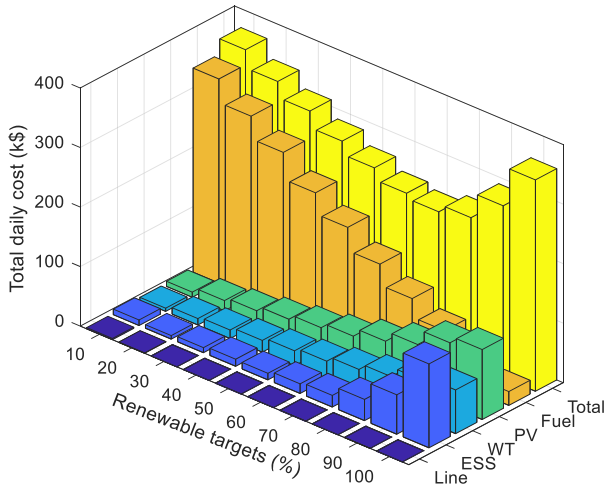

FIGURE 5. Daily costs of investment and operation with different renewable target.

push the accommodation of RES and reduce investment costs. In general, coordinated planning considering the interaction of source, grid, and ESS is the most economical scheme. From the perspective of engineering application, coordinated planning can make full use of the complementary advantages of multiple resource characteristics to ensure the economic operation of the power system. From mathematical optimization, joint optimization of multiple resources is equivalent to adding variables in the model to obtain a lower bound solution.

To verify the adaptability of the coordinated planning model, we studied the impact of different renewable target on the planning scheme, as shown in Figure 5.

The total daily cost shows a downward trend and then an upward trend with the increase of renewable target. The main reason is that the increased investment costs are gradually greater than the reduced TG operation costs as renewable target increases. Therefore, decision-makers must choose the right renewable target. Besides, it is not wise to restrict the spillover of RES strictly, which will lead to additional

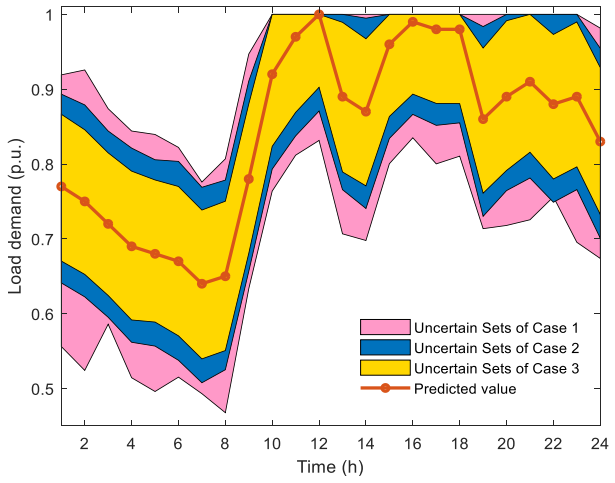

FIGURE 6. Confidence interval with different cases.

investment costs. As mentioned before, renewable target are different in time and spatially, and the benefits and costs of RES generation are changing. It is convenient to treat renewable target as parameters in the model. The coordinated planning model in this paper can easily give the planning scheme corresponding to renewable target.

C. EFFECTIVENESS OF TWO-STAGE ROBUST OPTIMIZATION

In this section, uncertain sets are constructed based on different sample sizes and confidence levels, and then the impact of uncertain sets on planning schemes is studied. The following three cases are tested as follows:

Case 1: an uncertain set U_1 based on 200 sample data at confidence level $\beta = 90\%$.

Case 2: an uncertain set U_2 based on 2000 sample data at confidence level $\beta = 90\%$.

Case 3: an uncertain set U_3 based on 2000 sample data at confidence level $\beta = 80\%$.

We assume that forecasting errors of load and RES follows normal distribution to generate scenarios of the uncertain demand and production. Taking load as an example, we set the covariance as 0.07 of its basic scenario values. Given a sample size and confidence level, the uncertain set of load demand can be obtained by applying data-driven modeling methods, as shown in Figure 6.

It can be seen from Figure 6, that the increase of sample size can reduce the width of uncertainty interval, and the decrease of confidence level can reduce the width of uncertainty interval (i.e. $U_1 > U_2 > U_3$). WT and PV power have similar trends, which will not be discussed here.

To compare with the example of the preceding section, the renewable target are also set as 10% of the load demand. We simply deal with an uncertain budget and set them to the maximum. Let $\Gamma_{d,s} = \Gamma_{w,s} = \Gamma_{pv,s} = 33$ and $\Gamma_{d,t} = \Gamma_{w,t} = \Gamma_{pv,t} = 24$. The planning results are shown in Table 5.

RES consumption in all cases is 860.3 MWh, 849.1 MWh, and 833.6 MWh, respectively. Such a result is caused by

TABLE 5. Comparison of schemes with different case.

	Case 1	*Case 2*	*Case 3*
Line	21-22	6-8, 15-23	6-8, 15-23
ESS	8(24), 15(15), 26(9), 28(2), 30(8)	8(23), 21(19), 26(2), 30(2)	9(2), 11(2), 21(22), 25(3), 30(9)
WT	8(10), 15(8), 25(3)	8(2), 21(17), 26(2)	21(14), 24(2), 26(2)
PV	8(19), 15(8), 18(4), 26(4)	8(21), 21(12), 26(2)	8(5), 10(4), 17(3), 21(16), 24(2)

TABLE 6. Daily costs comparison of schemes with different cases.

Cost($)	*Case 1*	*Case 2*	*Case 3*
Line	836	1278	1278
ESS	49206	39020	32241
WT	12533	12533	10743
PV	20051	20047	17188
Fuel	390224	383319	375651
Start-up	1560	1560	1560
Penalty	0	0	0
Total	474410	457757	437101

the difference of load uncertain sets. In *Case 1*, the installed capacity and spillover of RES are 310 MW and 617.1 MWh, respectively. In *Case 2*, the installed capacity and spillover of RES are 310 MW and 764.4 MWh, respectively. In *Case 3*, the installed capacity and spillover of RES are 360 MW and 635.9 MWh, respectively. It is not difficult to find that the installed capacity of RES in *Case 1* and *Case 2* is equal, and the RES consumption in *Case 1* is larger than that in *Case 2*. Be careful not to be confused by this result, which only represents part of the investment cost and does not include transmission lines and ESS investment as well as operation cost. The result of *Case 1* is conservative and the total daily cost is higher than that of *Case 2*. The daily cost of the schemes are given in Table 6.

Data in Table 6 show that the investment costs and operation costs of *Case 1*, *Case 2*, and *Case 3* are decreasing gradually. We are confident to conclude that the sample size is inversely proportional to the range of uncertain sets and the confidence interval is proportional to the range of uncertain sets, and the worst-case situation of U_3 are much more likely than those of U_1 and U_2. As a result, the conservativeness of the three planning schemes is gradually reduced, and the risk of failing to achieve renewable target is gradually increased.

Besides, the advantage of ARO over deterministic method is verified by power system operation simulation. *Scheme 1* and *Case 1* are tested based on 2000 randomly generated scenarios. The amount of unserved load for each scenario is given in Figure 7.

In *Scheme 1*, the average amount of unserved load is 13.1 MWh, and the probability of unserved load is 80.7%. In *Case 1*, the probability of unserved load is zero. The amount of renewable spillover for each scenario is given in Figure 8.

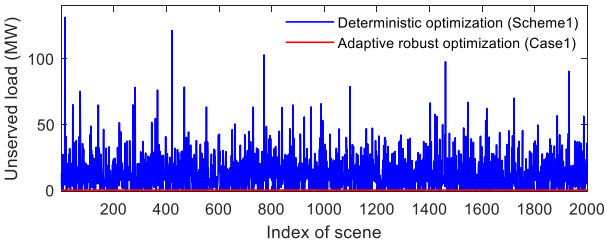

FIGURE 7. The amount of unserved load for Scheme 1 and Case 1.

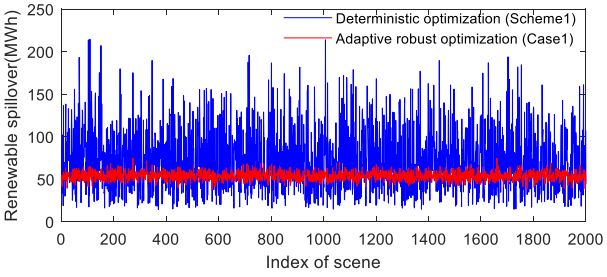

FIGURE 8. The amount of renewable spillover for Scheme 1 and Case 1.

The average amount of renewable spillover for *Scheme 1* and *Case 1* is 72.8 MWh and 54.0 MWh, respectively. The standard deviation of renewable spillover for *Scheme 1* and *Case 1* is 35.8 and 5.0, respectively.

From the comparison above, the advantages of ARO (*Case 1*) can be seen clearly. Although the investment cost of ARO is higher than that of deterministic optimization (*Scheme 1*), the risk of unserved load and renewable spillover of *Case 1* is lower than that of *Scheme 1* in power system operation.

D. ARO WITH MULTIPLE UNCERTAIN SETS

In this section, the sensitivity of planning cost to uncertain budget parameters is studied, which demonstrates the advantages of multiple uncertain set modeling techniques. The following two cases are tested as follows:

Case 4: The uncertain set U_1 and the uncertain set U_2 are considered, and the coefficients of the two uncertain sets are set according to the sample size, i.e. (1/11, 10/11).

Case 5: The uncertain set U_2 and the uncertain set U_3 are considered, and the coefficients of the two uncertain sets are set according to the confidence level, i.e. (9/17, 8/17).

The renewable target are set as 10%. Let $\Gamma(\Gamma_{d,t}, \Gamma_{w,t}, \Gamma_{pv,t})$ be the uncertain budget of load, wind and photovoltaic. We gradually increase the uncertain budget from 0 to 24, where steps size of $\Gamma_{d,t}$, $\Gamma_{w,t}$ and $\Gamma_{pv,t}$ are 4, 4 and 2, respectively. The total daily costs of the schemes are given in Figure 9.

With the increase of uncertain budget, the uncertain set becomes larger and the total daily cost increases. When the uncertain budget is set to $\Gamma(0,0,0)$, the coordinated planning model based on ARO degenerates into a deterministic problem. All cases are the same as *Scheme 1*, and the total cost is 368352 $. When the uncertain budget is set to $\Gamma(24,24,12)$, the daily cost of five cases is 474 k$, 458 k$, 437 k$, 468 k$,

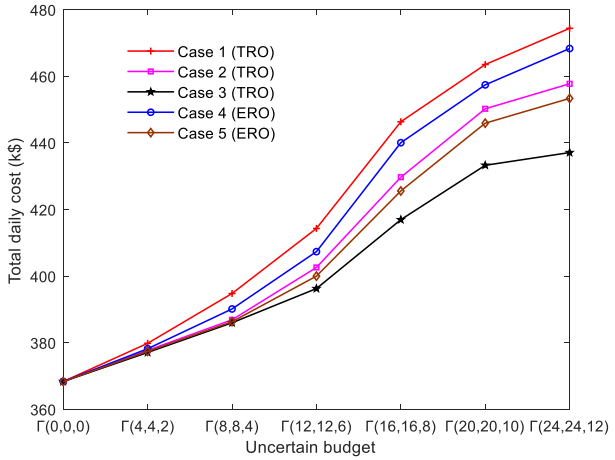

FIGURE 9. Total daily costs of schemes in different uncertain budget.

and 453 k$, respectively. The uncertainty set is the largest, and the total cost is more sensitive to an uncertain budget. Therefore, the sensitivity of *Case 4* to the uncertain budget is between *Case 1* and *Case 2*, while that of *Case 5* is between *Case 2* and *Case 3*. Although the weight coefficient of U_1 is set very small, *Case 4* gradually approaches *Case 1* as the total cost of *Case 1* increases. Note that the impact of uncertain sets of load and RES on total costs is different. Contrary to RES, the size of the load uncertainty set is proportional to the total cost. It is easy to understand that increasing demand and reducing productivity will increase capital investment.

Besides, *Case 1*, *Case 2*, and *Case 3* (TRO) represents the traditional RO scheme considering single uncertain set. *Case 4* and *Case 5* (ERO) represents the extended RO scheme considering multiple uncertain sets. From the above analysis, the advantages of ERO can be seen clearly. Considering multiple uncertain sets can reduce the sensitivity of decision-making scheme to uncertainty set.

VI. CONCLUSION

In this paper, we proposed an extend two-stage robust coordinated planning model to support the efficient achievement of renewable target considering economy of the system by accounting for the interaction between source, grid, and ESS. We perform a set of numerical experiments on coordinated planning models to illustrate modeling strength and economic outcomes under different uncertainty sets. Simulation results show that:

(1) Although RES can reduce system operation cost, the investment cost of the system also increases. The growth of the renewable target should be coordinated with the GEP, TEP, and ESS plan to properly accommodate renewable energy and possibly reduce investment and operational costs.

(2) Multiple uncertain sets, uncertain budget, and data-driven modeling techniques can strengthen uncertainty sets description and reduce the conservativeness of decision-making schemes. The design of more accurate and friendly uncertainty sets can achieve a trade-off between the computational burden and accuracy.

TABLE 7. Parameters of candidate transmission lines.

f_bus	*t_bus*	*x*(p.u.)	L(km)	*f_bus*	*t_bus*	*x*(p.u.)	L(km)
1	2	0.06	120	15	18	0.22	52
1	3	0.19	140	18	19	0.13	54
2	4	0.17	80	19	20	0.07	74
3	4	0.04	140	10	20	0.21	78
2	5	0.20	150	10	17	0.08	75
2	6	0.18	80	10	21	0.07	68
4	6	0.04	120	10	22	0.15	65
5	7	0.12	90	21	22	0.02	70
6	7	0.08	140	15	23	0.20	52
6	8	0.04	55	22	24	0.18	58
6	9	0.21	90	23	24	0.27	55
6	10	0.56	60	24	25	0.33	53
9	11	0.21	82	25	26	0.38	60
9	10	0.11	85	25	27	0.21	55
4	12	0.26	80	28	27	0.40	65
12	13	0.14	70	27	29	0.42	50
12	14	0.26	75	27	30	0.60	50
12	15	0.13	72	29	30	0.45	50
12	16	0.20	62	8	28	0.20	60
14	15	0.20	50	6	28	0.06	65
16	17	0.19	55				

(3) ARO scheme with high investment cost can lower the risk of unserved load and renewable spillover.

Finally, further extensions with more focus on methods that analytically make use of existing data, such as construct computationally friendly uncertainty sets in machine learning fashion are worth a deep study. Besides, the impact of financial incentives on the investment behavior of market participants is in a perfect competition market environment is also worth study.

APPENDIX

See Table 7 Here.

REFERENCES

[1] F. R. Badal, P. Das, S. K. Sarker, and S. K. Das, "A survey on control issues in renewable energy integration and microgrid," *Protection Control Mod. Power Syst.*, vol. 4, no. 1, pp. 87–113, Dec. 2019.
[2] B. Mohandes, M. S. E. Moursi, N. Hatziargyriou, and S. E. Khatib, "A review of power system flexibility with high penetration of renewables," *IEEE Trans. Power Syst.*, vol. 34, no. 4, pp. 3140–3155, Jul. 2019.
[3] X. Chen, J. Lv, M. B. Mcelroy, X. Han, C. P. Nielsen, and J. Wen, "Power system capacity expansion under higher penetration of renewables considering flexibility constraints and low carbon policies," *IEEE Trans. Power Syst.*, vol. 33, no. 6, pp. 6240–6253, Nov. 2018.
[4] N. E. Koltsaklis and A. S. Dagoumas, "State-of-the-art generation expansion planning: A review," *Appl. Energy*, vol. 230, pp. 563–589, Nov. 2018.
[5] A. Moreira, D. Pozo, A. Street, and E. Sauma, "Reliable renewable generation and transmission expansion planning: Co–optimizing system's resources for meeting renewable targets," *IEEE Trans. Power Syst.*, vol. 32, no. 4, pp. 3246–3257, Jul. 2017.
[6] M. Peker, A. S. Kocaman, and B. Y. Kara, "Benefits of transmission switching and energy storage in power systems with high renewable energy penetration," *Appl. Energy*, vol. 228, pp. 1182–1197, Oct. 2018.
[7] J. A. Taylor, "Financial storage rights," *IEEE Trans. Power Syst.*, vol. 30, no. 2, pp. 997–1005, Mar. 2015.
[8] A. Nikoobakht and J. Aghaei, "Integrated transmission and storage systems investment planning hosting wind power generation: Continuous-time hybrid stochastic/robust optimisation," *IET Gener., Transmiss. Distrib.*, vol. 13, no. 21, pp. 4870–4879, Nov. 2019.

[9] I. Sharan and R. Balasubramanian, "Generation expansion planning with high penetration of wind power," *Int. J. Emerg. Electr. Power Syst.*, vol. 17, no. 4, pp. 401–423, Aug. 2016.
[10] F. Luo, K. Meng, Z. Y. Dong, Y. Zheng, Y. Chen, and K. P. Wong, "Coordinated operational planning for wind farm with battery energy storage system," *IEEE Trans. Sustain. Energy*, vol. 6, no. 1, pp. 253–262, Jan. 2015.
[11] N. Zhang, Z. Hu, B. Shen, S. Dang, J. Zhang, and Y. Zhou, "A source-grid-load coordinated power planning model considering the integration of wind power generation," *Appl. Energy*, vol. 168, pp. 13–24, Apr. 2016.
[12] M. Asensio, P. Meneses De Quevedo, G. Munoz-Delgado, and J. Contreras, "Joint distribution network and renewable energy expansion planning considering demand response and energy storage—Part I: Stochastic programming model," *IEEE Trans. Smart Grid*, vol. 9, no. 2, pp. 655–666, Mar. 2018.
[13] L. Baringo and A. Baringo, "A stochastic adaptive robust optimization approach for the generation and transmission expansion planning," *IEEE Trans. Power Syst.*, vol. 33, no. 1, pp. 792–802, Jan. 2018.
[14] E. Gil, I. Aravena, and R. Cardenas, "Generation capacity expansion planning under hydro uncertainty using stochastic mixed integer programming and scenario reduction," *IEEE Trans. Power Syst.*, vol. 30, no. 4, pp. 1838–1847, Jul. 2015.
[15] S. Dehghan, N. Amjady, and A. J. Conejo, "Adaptive robust transmission expansion planning using linear decision rules," *IEEE Trans. Power Syst.*, vol. 32, no. 5, pp. 4024–4034, Sep. 2017.
[16] A. Nikoobakht, J. Aghaei, T. Niknam, M. Shafie-khah, and J. P. S. Catalao, "Smart wire placement to facilitate large–scale wind energy integration: An adaptive robust approach," *IEEE Trans. Sustain. Energy*, vol. 10, no. 4, pp. 1981–1992, Oct. 2019.
[17] E. Spyrou, J. L. Ho, B. F. Hobbs, R. M. Johnson, and J. D. Mccalley, "What are the benefits of co–optimizing transmission and generation investment? Eastern interconnection case study," *IEEE Trans. Power Syst.*, vol. 32, no. 6, pp. 4265–4277, Nov. 2017.
[18] G. Li, G. Li, and M. Zhou, "Model and application of renewable energy accommodation capacity calculation considering utilization level of inter-provincial tie-line," *Protection Control Mod. Power Syst.*, vol. 4, no. 1, pp. 1–12, Dec. 2019.
[19] S. Dehghan and N. Amjady, "Robust transmission and energy storage expansion planning in wind farm–integrated power systems considering transmission switching," *IEEE Trans. Sustain. Energy*, vol. 7, no. 2, pp. 765–774, Apr. 2016.
[20] Y. An and B. Zeng, "Exploring the modeling capacity of two–stage robust optimization: Variants of robust unit commitment model," *IEEE Trans. Power Syst.*, vol. 30, no. 1, pp. 109–122, Jan. 2015.
[21] A. Baíllo, A. Cuevas, and A. Justel, "Set estimation and nonparametric detection," *Can. J. Statist.*, vol. 28, no. 4, pp. 765–782, Dec. 2000.
[22] J. Frey, "Confidence bands for the CDF when sampling from a finite population," *Comput. Statist. Data Anal.*, vol. 53, no. 12, pp. 4126–4132, Oct. 2009.
[23] C. Duan, L. Jiang, W. Fang, and J. Liu, "Data–driven affinely adjustable distributionally robust unit commitment," *IEEE Trans. Power Syst.*, vol. 33, no. 2, pp. 1385–1398, Mar. 2018.
[24] A. Velloso, A. Street, D. Pozo, J. M. Arroyo, and N. G. Cobos, "Two-stage robust unit commitment for co-optimized electricity markets: An adaptive data-driven approach for scenario-based uncertainty sets," *IEEE Trans. Sustain. Energy*, to be published, doi: 10.1109/TSTE.2019.2915049.
[25] C. Ning and F. You, "Data–driven adaptive robust unit commitment under wind power uncertainty: A Bayesian nonparametric approach," *IEEE Trans. Power Syst.*, vol. 34, no. 3, pp. 2409–2418, May 2019.
[26] X. Xu, Z. Yan, M. Shahidehpour, Z. Li, M. Yan, and X. Kong, "Data–driven risk–averse two–stage optimal stochastic scheduling of energy and reserve with correlated wind power," *IEEE Trans. Sustain. Energy*, vol. 11, no. 1, pp. 436–447, Jan. 2020.
[27] Z. Shi, H. Liang, S. Huang, and V. Dinavahi, "Distributionally robust chance–constrained energy management for islanded microgrids," *IEEE Trans. Smart Grid*, vol. 10, no. 2, pp. 2234–2244, Mar. 2019.
[28] R. Garcia-Bertrand and R. Minguez, "Dynamic robust transmission expansion planning," *IEEE Trans. Power Syst.*, vol. 32, no. 4, pp. 2618–2628, Jul. 2017.
[29] A. Nikoobakht, J. Aghaei, H. Farahmand, V. Lakshmanan, and M. Korpås, "Flexibility of controllable power transformers for managing wind uncertainty using robust adjustable linearised optimal power flow," *IET Renew. Power Gener.*, vol. 13, no. 2, pp. 262–272, Feb. 2019.
[30] B. Zeng and L. Zhao, "Solving two-stage robust optimization problems using a column-and-constraint generation method," *Oper. Res. Lett.*, vol. 41, no. 5, pp. 457–461, Sep. 2013.
[31] T. Ding, S. Liu, W. Yuan, Z. Bie, and B. Zeng, "A two–stage robust reactive power optimization considering uncertain wind power integration in active distribution networks," *IEEE Trans. Sustain. Energy*, vol. 7, no. 1, pp. 301–311, Jan. 2016.
[32] R. W. Ferrero, S. M. Shahidehpour, and V. C. Ramesh, "Transaction analysis in deregulated power systems using game theory," *IEEE Trans. Power Syst.*, vol. 12, no. 3, pp. 1340–1347, Aug. 1997.

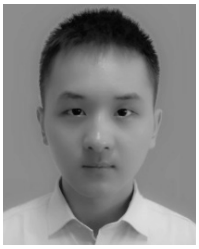

KUNPENG TIAN received the M.S. degree in electrical engineering from the University of Shanghai for Science and Technology, Shanghai, China, in 2018, where he is currently pursuing the Ph.D. degree. His research interests include power system operation and investment planning.

WEIQING SUN received the B.S., M.S., and Ph.D. degrees in electrical engineering from Shanghai Jiao Tong University, Shanghai, China, in 2007, 2009, and 2013, respectively. He is currently an Associate Professor with the University of Shanghai for Science and Technology, Shanghai. His current research interests include renewable energy, power system planning, and optimization theory.

DONG HAN received the Ph.D. degree in electrical engineering from Shanghai Jiao Tong University, Shanghai, China, in 2016. He is currently a Lecturer with the University of Shanghai for Science and Technology, Shanghai. His current research interests include electricity market and optimization theory.

CE YANG received the M.S. degree in electrical engineering from the University of Shanghai for Science and Technology, Shanghai, China, in 2019, where he is currently pursuing the Ph.D. degree. His research interests include power system economics and robust optimization.